EXPERIMENTAL STUDY ON THE PRESSURE DROP OF A SUPERCRITICAL FLUID IN A PLATE HEAT EXCHANGER

D.W. DE HAAS
Delft University of Technology, Department of Radiation, Radionuclides and Reactors
The Netherlands
D.W.DeHaas@tudelft.nl

P. VAN DER BAAN
Delft University of Technology, Department of Radiation, Radionuclides and Reactors
The Netherlands
P.Vanderbaan@tudelft.nl

CHRISTOPHE T'JOEN
Delft University of Technology, Department of Radiation, Radionuclides and Reactors
The Netherlands
c.g.a.tjoen@tudelft.nl

Abstract
Because of their unique fluid properties which show very sharp gradients if the temperature is near the (pseudo)critical point, supercritical fluids are being used more frequently today in a range of industrial applications. As a result there is a strong need for the development of effective heat exchangers to control the temperature of these media. Because of their small footprint and excellent performance in both single and multi-phase applications, compact plate heat exchangers are being considered as a main option. As a first exploratory study, a standard plate heat exchanger design from SWEP (B16DW with 14 parallel channels) is studied here using supercritical Freon R23. This fluid was selected as a scaling fluid for supercritical water. The pressure drop was determined for a varying flow rate and for an isothermal flow and for a varying inlet temperature. This value was converted to a friction factor. The results indicate that despite the strong property variations which occur, the friction factors determined for flows with strongly varying properties, agree well with those for an isothermal flow.

Keywords: supercritical fluid, plate heat exchanger, pressure drop

INTRODUCTION

Despite the harsh requirements a supercritical fluid imposes on applications (due to high pressure, temperature, possible strong corrosion…), a strong drive exists to use supercritical fluids in a range of different applications. One of the prime movers is the power cycle for electricity generation (Rankine cycle with a turbine, geothermal systems…). By raising the working pressure and temperature of the fluid, the cycle efficiency can be increased (Carnot law). This has lead to the development of (ultra-) supercritical coal fired electricity plants with a steam pressure as high as 330 bar which are currently in operation worldwide (e.g. in Japan, Denmark, the United States…, Susta (2004)). Using supercritical fluids has also been proposed for the power cycles of the Generation IV advanced nuclear reactor designs, both in the primary loop (the Supercritical Water Reactor – SCWR, Buongiorno and MacDonald

(2003)), and in the secondary loop (using supercritical CO_2 as power fluid in a Brayton cyle for the sodium fast reactor, Cha et al. (2009)). Using supercritical fluids not only provides an increased thermal efficiency, but can also help reduce the complexity of the plant (due to avoiding phase separation), which helps to cut plant investment costs. On a smaller power scale there has been a lot of interest to use supercritical CO_2 as a natural refrigerant instead of Freon based hydrocarbons in compression cooling cycles as part of the ongoing struggle to reduce greenhouse gas emissions, see e.g. Kim et al. (2003). Commercial application of this technology already exists for e.g. large supermarkets. Another future application of supercritical fluids are the 'organic rankine cycles' (ORC) which aim at energy recovery from low temperature heat streams which are currently being discarded. Schüster et al. (2010) showed that by using a transcritical cycle, an improvement of about 8% in the cycle efficiency could be obtained compared to subcritical conditions due to the higher exergetical efficiency.

Another important application for supercritical fluids is as a solvent for chemical reactions in the oil, food, pharmaceutical and biochemical industries, and this because of their superior mass transfer properties, mixing capabilities compared to liquid solvents and the ability to 'tune' separation: due to the strong density gradient near the pseudo-critical point very small changes in temperature or pressure can result in separation of the dissolved materials which allows for a very strict process control, see e.g. Malek Abbaslou et al. (2009). Typical applications are the dyeing of delicate fabrics, extraction of essential oils and caffeine, etc. Supercritical water is also used for the oxidation of harmful organic compounds contained in aqueous waste, a process which is known as SCWO, supercritical water oxidation, Schmieder and Abeln (1999).

The short introduction above shows that supercritical fluids are widely used today in modern industrial applications. It is also expected that in the coming decades the number of applications that make use of this type of fluids will increase, as they allow to obtain better products and to operate processes more effectively or in a more efficient way. This will help with the global struggle to reduce emissions and to raise energy efficiency, which is in sync with the European 20 20 20 milestones. In general process applications, heat exchangers are needed to control the supercritical fluid temperature by either heating or cooling. For some processes a very tight temperature control is even required. Because of their compact structure and high heat transfer potential, plate heat exchangers are a typical candidate for these kinds of processes. Unfortunately very little data is available in open literature on the pressure drop and heat transfer of a supercritical fluid through such a plate heat exchanger. This paper will present some new data. In the next paragraphs we'll first introduce plate fin heat exchangers, supercritical fluids and the experimental setup, before presenting the final results.

Plate heat exchangers (PHE) are devices composed of stacked plates separating the hot and cold fluid streams. The plates are either brazed or welded, or have gaskets and are held together by a frame. PHE are commonly used in the chemical and food industry and increasingly in many other applications. Compared to competing designs like shell-and-tube heat exchangers, PHE offer high effectiveness at very compact size and are available in a wide variety. An advantage of a gasketed PHE is the ease of maintenance and the extensibility, since gasketed plates can be dis- and re-assembled in short time for cleaning and plates can be added to adapt to higher heat or cooling loads. This type of PHE is schematically shown in Fig 1 A. Because of their high surface-to-volume ratio, PHE belong to the group of compact heat exchangers, see Shah and Sekulic (2003). PHE owe their high

heat transfer effectiveness not only to the large surface area, but also to the specific design of the plates. These feature corrugations, usually sinusoidal wave shaped, commonly arranged in "chevron patterns" with opposite pitch angles in a plate pair. The surface structures force the flow in the channels into certain intersecting flow paths and induce high levels of turbulence. The angle of the chevron pattern is a decisive factor for heat transfer performance and pressure drop. With increasing angle, the heat transfer increases due to the stronger mixing, but it is accompanied with a sharp gain in pressure drop. The hot and cold side fluids usually stream in counterflow arrangement to minimize the approach temperature. PHE are mostly used for liquid fluids with low viscosity in single-phase flow. This type of heat exchanger is also becoming common for evaporators and condensers in HVAC&R applications when liquid secondary fluids are involved, e.g. as chillers or for water-cooled condensers.

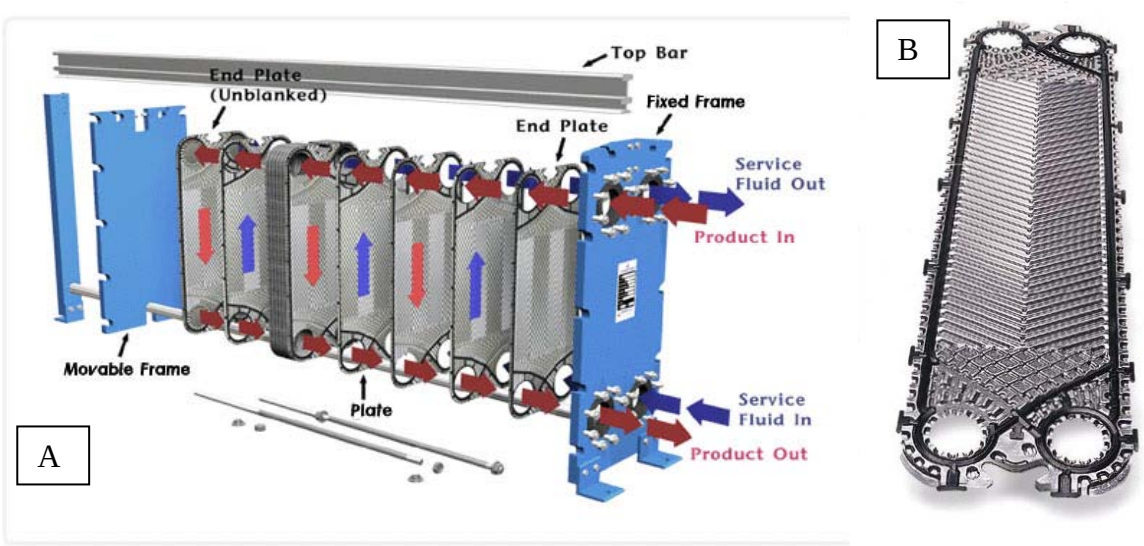

Figure 1: A. Schematic illustration of a gasketed PHE, B: detailed view of a single plate showing the complex surface geometry, the chevron pattern.

Despite the widespread use of PHE, only limited detail is known from experiments about their fluid dynamics and subsequently the local heat transfer inside. This is in part due to the very complex geometry, making access to the walls very difficult. A major contribution is due to Stasiek et al. (1996) who investigated the distributions of local Nusselt numbers on cross-corrugated surfaces. The studied geometry is very similar to the structure in common PHE. Their results include Nusselt number maps of unitary cells of the cross-corrugated structure for various angles and Reynolds numbers. Their experiments were supplemented with CFD simulations that gave insight into the swirling flow regime (Ciofalo et al. 1996). Freund and Kabelac (2010) provide an overview of previous experimental and numerical work aimed at understanding the flow mechanics and determining the local heat transfer coefficients. They focussed on determining the local heat transfer coefficients, and were able to reveal experimentally the very complex heat transfer patterns that occur due to the swirling fluid travelling in between and across the troughs, with local maxima.

Because of their strong surface corrugation, PHE suffer a large pressure drop. This is particularly penalizing in multiphase flows where the fluid undergoes density variations. As a result, a number of authors have studied optimizing the chevron pattern to reduce the pressure drop, e.g. Arsenyeva et al. (2010) varied the gap spacing in between subsequent chevrons to reduce the total pressure drop. Their final experiment (based on a design process) revealed a considerable reduction (about 40%) in pressure loss for the condensing media. At the same

time, the overall heat transfer remained high. This indicates that further improvements can still be made in the PHE design.

A lot of different studies have been published presenting thermo-hydraulic data for PHE units, and these usually show a large scatter even for cases that are quite similar. The plate corrugation shape has the largest impact on the thermal and hydraulic performance of PHEs. Most recent attempts to generalize correlations for pressure drop and heat transfer in PHE channels were made by Dović et al. (2009) and by Khan et al. (2010). Both these papers explored the impact of the different geometric parameters of the PHE on the resulting pressure drop and heat transfer.

Dović et al. (2009) developed a theoretical model based on the idea of developing flow in sine shaped ducts. Based on flow visualization studies they differentiated between two velocity components: indicate the existence of basically two flow components – the longitudinal one, moving in a helix flow pattern in the main direction of the flow and the furrow component, following the direction of the corrugation. The relative influence of the two components determines whether the flow pattern is considered as wavy longitudinal or as furrow flow. In general, flow in channels with a chevron angle larger than 60° will be predominantly wavy longitudinal, while in channels with a chevron angle smaller than 45° the furrow flow pattern prevails. Beside the chevron angle, considered as the most influencing parameter, other parameters like the aspect ratio and flow velocity were shown to have significant impact on the relative importance of each flow component. Dović et al. (2009) developed a model to describe the transition between these two regimes, but compared to experimental data, the results showed significant deviation (more than 40% for some cases), in particular for the friction factors. They also notated that there are many uncertainties in this model, e.g. the impact of the variable header geometries is not considered. Also they found that as the viscosity changes (e.g. by using glycol/water instead of water), different flow velocities may produce different flow patterns at the same *Re* which finally results in different values of the Nusselt number and friction factor. This would call for redefinition of *Re* number and/or introduction of some other dimensionless quantity in presentation of the thermal–hydraulic characteristics, which would better reflect actual flow pattern. Considering the sharp change in fluid properties that occurs in supercritical fluids during heating or cooling, and the uncertainty on the flow regime approach, this model was not further considered.

SUPERCRITICAL FLUIDS

A supercritical fluid is defined as a substance above its critical temperature T_c and critical pressure P_c. The critical point (T_c, P_c) represents the highest temperature and pressure at which the substance can exist as a vapor and a liquid in equilibrium, i.e. the top of the vapor dome. Above this point the substance exists as a fluid without distinct phases. Figure 2 shows the P-v diagram for water and indicates the areas where it exists as a liquid, a gas or a supercritical fluid. The black solid lines are the saturated liquid and vapor line, representing the temperatures and pressure where two phases exist in equilibrium. By increasing the temperature at a given pressure below P_c the liquid reaches the saturated liquid line and starts to boil. A mixture of vapor and liquid is formed. By adding an amount of energy equal to the enthalpy of vaporization, all of the liquid will be transformed into gas. If we move upwards along the boiling curve, increasing both pressure and temperature, the liquid will become less dense due to thermal expansion and the gas will become denser as the pressure rises. Eventually the densities of both phases converge and the distinction between gas and liquid

disappears, having reached the critical point. The critical point for water occurs at T_c = 373.95 °C, P_c = 220.64 bar.

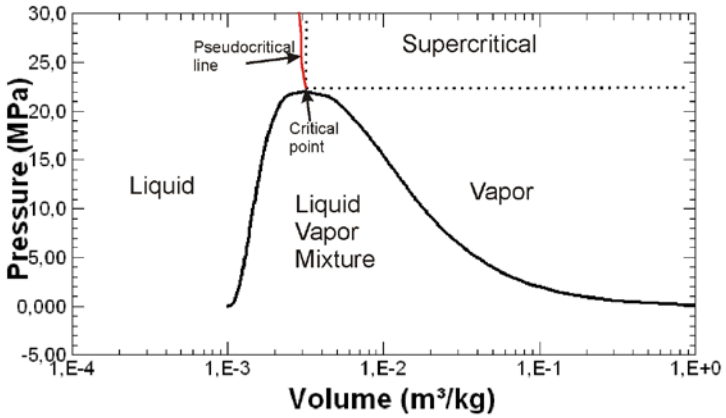

Figure 2: P-v diagram of water, indicating the different phases.

Near the critical point experiences supercritical fluids experience very sharp changes in the transport properties (density, viscosity, thermal conductivity, Prandtl number…). Quite remarkable is the behaviour of the specific heat capacity, which shows a very sharp rise to a peak value before dropping off again (see Fig. 3). The temperature at which this peak occurs is the 'pseudo-critical temperature' T_{pc}. As the pressure increases so does the pseudo-critical temperature. At higher pressures the property changes become more gradual but they remain pronounced. These changes have a significant impact on the transport behaviour (e.g. convective heat and mass transfer) in these fluids as they can provide unique combinations such as a liquid like density with gas-like transport properties. Also, because of the strong peak in the specific heat capacity, the fluid is able to absorb considerably more energy without a strong increase of the temperature. At the Delft University of Technology a supercritical loop was built to study the SCWR, specifically the stability of the entire loop while operating using natural circulation, see Rohde et al. (2011). The plate heat exchanger considered here is part of this loop. In the subsequent section the loop will be briefly described, as well as the heat exchanger.

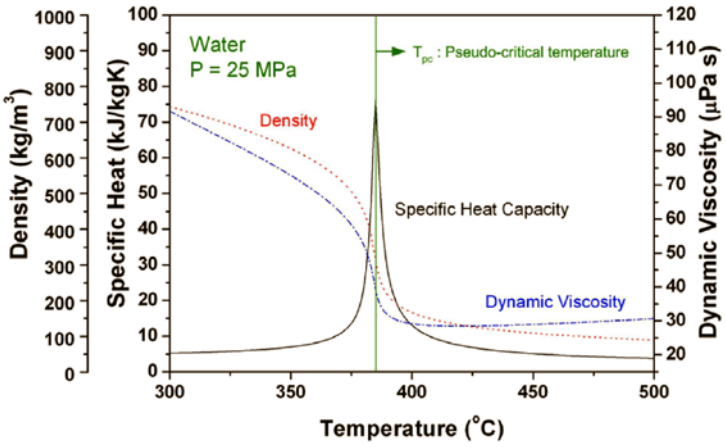

Figure 3: Illustration of the transport property variation near the pseudo-critical point (water, 25 MPa, T_{pc} = 384.8 °C).

EXPERIMENTAL SETUP

In order to reduce the pressure and temperature level and the power requirements imposed by the supercritical water to more suitable lab values, a scaling fluid was used. Rohde et al. (2011) describe the scaling procedure based on the conservation of the Froude number and the friction distribution. After comparison of a large number of different fluids, Freon R23 (CHF_3) was selected as the scaling fluid based on the power requirement, the temperature (the pseudo-critical temperature is only 33°C), the pressure (5.7 MPa) and safety (non flammable). The non-dimensional fluid properties agree well, with a maximum deviation of 8% for the density far away from the pseudo-critical point. Some relevant pseudo-critical fluid properties and scaling values are indicated in Table 1.

Table 1: Comparison of selected pseudocritical properties of H_2O and R23 and the considered scaling rules, Rohde et al. (2011)

	R23	H_2O	Scaling factor	
Pressure (MPa)	5.7	25	Length	0.191
Temperature (°C)	33.2	384.9	Diameter	1.06
Density (kg/m³)	537	316.82	Power	0.0788
Enthalpy (kJ/kg)	288.3	2152.9	Mass flux	0.74
Core inlet temperature (°C)	-21	280	Time	0.438
Core exit temperature (°C)	105	500		

Based on the derived scaling rules, an experimental facility has been constructed, named 'DeLight' (Delft Light water reactor facility). A schematic drawing is shown in Fig. 4 and some of the dimensions are listed. The loop is constructed using stainless steel tubing (6mm ID for the core sections, 10 mm ID for the riser and downcomer). The total height of the loop is 10 m. Up to 18 kW of heating (twice the scaled power requirement) can be added at the bottom of the loop. This heating is done electrically by sending a current through the tubes (up to 600A per core element using Delta SM15-200 power units). Each heating section is electrically insulated from the rest of the setup using a PEEK ring mounted in between 2 flanges. To provide a stable pressure level, a buffer vessel is present at the top of the loop which has a moveable piston (Parker Series 5000 Piston Accumulator) connected to a nitrogen gas cylinder. By positioning this piston higher or lower the pressure level in the loop can be set at 5.7 MPa. Two heat exchangers (labeled HX in Fig. 4) are mounted in series at the top section of the loop to extract the heating power and to set the inlet conditions. In the first one, the SWEP plate fin heat exchanger which is studied here, cooling water is used at the secondary side with a constant flow rate of 0.49 l/s and an inlet temperature of about 17°C (coming from the building water supply). This heat exchanger usually manages to cool the supercritical R23 down to almost 17°C (indicating it is relatively oversized). It has 14 parallel channels and is mounted horizontally. In the second unit, which is a welded plate fin heat exchanger from Vahterus Oy© R507a flows at the secondary side with a variable expansion pressure. This allows to set a variable inlet temperature for the loop.

The loop contains a large number of sensors to closely monitor the thermohydraulics. At the top and bottom absolute pressure sensors are presents (p symbol in Fig. 4, ± 0.15%). Thermocouples (T symbol in Fig. 4, ± 0.2K) are present at the inlet and exit of both fluid streams of the heat exchanger. This allows to monitor the heat rate. A differential pressure drop sensor is mounted over the heat exchanger, which allows to record the pressure drop over the unit. The individual thermocouple channels were calibrated carefully using 3 reference thermocouples which were calibrated over the entire temperature range by a

certified body. The R23 mass flow rate is imposed in the loop for these measurements using the pump mounted in the bottom. The R23 mass flow rate is measured using a coriolis mass flow meter (F symbol in Fig. 4, ± 0.25%). The cooling water flow rate is measured using an electromagnetic flow meter (max 0.6 l/s). The data acquisition system consists of a PC with one National Instruments PCI-6259 data acquisition card, connected to a National Instruments SCXI-1001 rack with two SCXI-1102B 32-channel amplifiers. This system is used for monitoring the experimental setup and for recording sensor signals. The measured and processed data are displayed on a PC screen which allows for continuous monitoring. Additionally, seven signals (three temperature values, two pressure values, and the R23 and cooling water flow rates) are connected to a separate stand-alone data acquisition system. This system is used for safety monitoring and will shut down the power supplies if one of the signals exceeds prescribed limits. A third PC is used to control the setup, setting the pressure level and the power input.

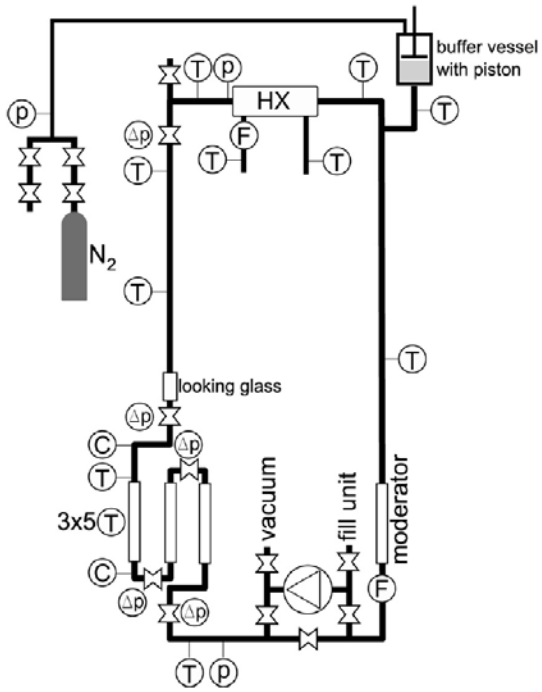

Heating section length: 0.8 m
Total height: 10.26 m

HX1: SWEP© B16DW U
Secondary side: water
secondary side flow rate: 0.49 l/s
secondary side Tin: ±18°C

HX2: Vahterus Oy© Q-Plate
Secondary side: R507a
secondary side flow rate: variable
secondary side Tin: variable (-40 to -5°C)

Pump: 3M Vanemag Pump with a magnetic rotor

Figure 4: Schematic of the DeLight facility with dimensions and equipment specifications.

EXPERIMENTAL PROCEDURE

The following procedure was used to determine the pressure drop data reported here. First, the pump was used to start the circulation in the loop. The pressure was then raised above the critical pressure by lowering the piston. Three types of measurements were performed: isothermal, with the heat exchanger cooling the fluid, and with the heat exchanger heating the fluid. For the second type of measurements, heating was added in the bottom of the loop, until the desired temperature was reached. By simultaneously controlling the position of the piston and slowly incrementing the added heat, the system was brought to the required testing conditions (5.7 MPa, and a specified inlet temperature). For the latter measurements, the cooling setup was turned on through the second heat exchanger. To control the inlet temperature, the expansion pressure on the secondary side of HX2 was set to -10°C or 0°C. To reach values in between or for finer control of the inlet temperature, a heater section was used. By adding more or less heat, the temperature could be controlled to within 0.2°C, and this was used to set the ‘cold’ temperatures (< 17°C). To judge if the system was stable, a

number of signals were monitored: three temperatures (core inlet and outlet and heat exchanger outlet): variation < 0.2 °C, and the absolute pressure variations in the loop (< 0.025 MPa). Once a steady state situation has been reached, the measurement was started. Over a period of five minutes the average pressure drop was recorded over the heat exchanger. One batch of measurements was repeated at the end of the measurement campaign to verify the repeatability.

RESULTS

Isothermal pressure drop measurements

To characterise the geometry of the plate fin heat exchanger, we define the hydraulic diameter D_h (Eq. (1)) as suggested by Shah and Focke (1988). This definition is commonly used by others, see e.g. Claesson (2004). Hereby b represents the distance between the plates (1.4 mm) and φ the surface enhancement ratio (estimated at 1.2 for this heat exchanger). The resulting hydraulic diameter is 2.33 mm, which is a typical value for PHE. The Reynolds number Re is defined using the mass flux and the hydraulic diameter, Eq. (2). To obtain the friction factor from the measured pressure drop, Eq. (3) is used. Note that the distance between the centre of the inlet and exit ports L_p (329 mm) is used as the reference length. Some other studies considered the full length of the heat exchanger, see Claesson (2004), but this distance is also a common reference. Also note that the friction factor is determined from the total pressure drop measurement, so it includes the effect of the inlet losses and exit regain. This is because there is no motivated model available to compute these discrete contributions. The mass flux is based on the minimal cross sectional area ($3.9\ 10^{-5}$ m²). An error analysis was performed, based on the procedures described by Moffat et al. (1988). Two times the standard deviation of the measured values was used as uncertainty estimate. An uncertainty of 0.1% was assumed on the density of R23, as obtained from the NIST Refprop database.

$$D_h = \frac{2b}{\varphi} \tag{1}$$

$$\mathrm{Re}_h = \frac{G \cdot D_h}{\mu} \tag{2}$$

$$f = \frac{\rho \cdot \Delta p \cdot D_h}{2 \cdot L_p \cdot G^2} \tag{3}$$

The results of the isothermal measurements are shown using black symbols in Fig. 5. As can be seen these data show the typical decreasing trend as Re_h increases. Note that a log-log scale is used. Often in heat exchanger data reduction, a power law regression is used to describe the Nusselt number or the friction factor. The results show that this would work reasonably well for the first part of the data, however, at higher Re_h, there seems to be a slight shift away from the power law (which would be a straight line in a log diagram). This could indicate a change in flow behaviour within the heat exchanger, but it is not possible to link to any other observation. The PHE geometry is known to result in flows that have a strong swirling component. This results in a very ‘early’ onset of turbulent flow, at Re_h between 10 and 500, Focke (1983). As such, it seems very unlikely this divergence indicates the onset of turbulence. The average uncertainty for the reported friction factors is 10.1%.

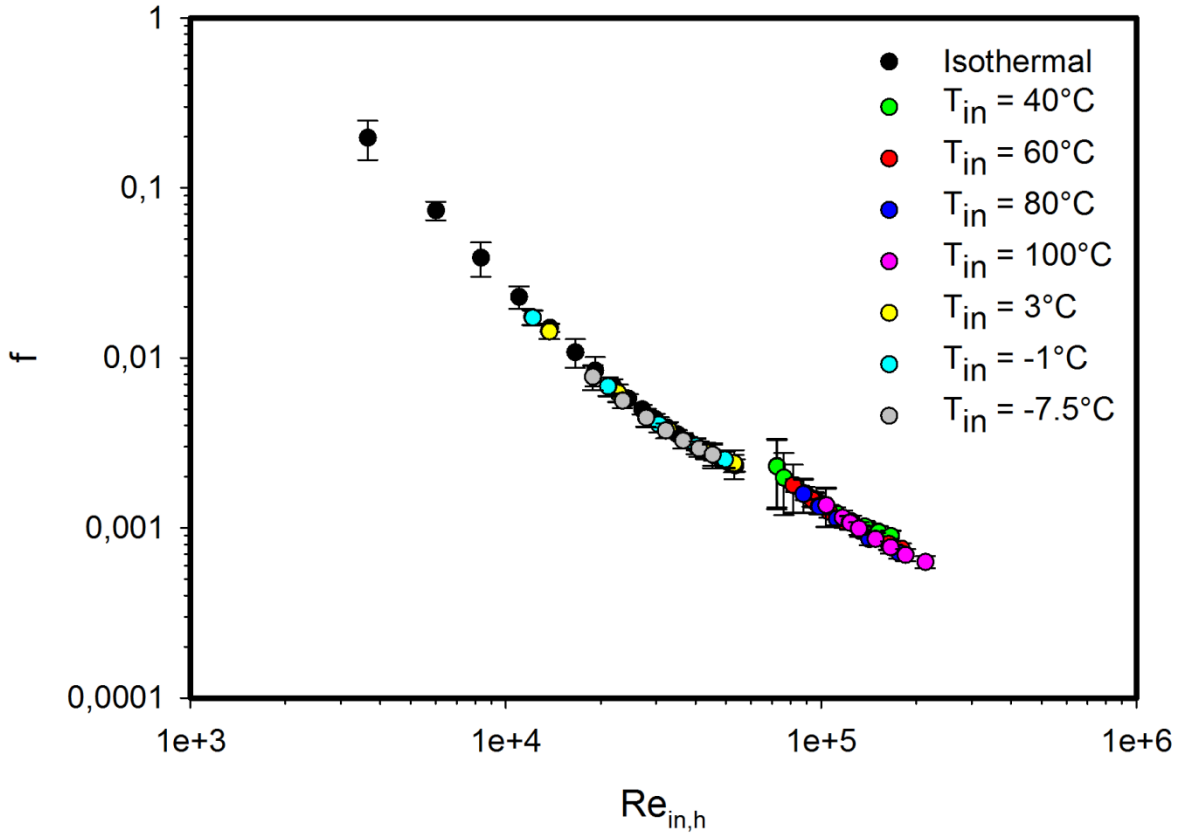

Figure 5: friction factors set out against Re_h.

Non-isothermal friction factors

Next a series non-isothermal pressure drop measurements were conducted. The inlet temperature was set to 40°C, 60°C, 80°C and 100°C. In these cases the supercritical fluid is cooled down in the heat exchanger. Three series were measured with an inlet temperature below 17°C, namely -7.5°C, -1°C and 3°C. The same equations were used to determine the friction factor, and the results are added to Fig. 5. To compute the substance properties, the inlet temperature was considered. As can be seen, the results agree well with the isothermal friction factors. The series measured at higher temperature have a higher Reynolds number as the viscosity shows a significant drop, see Fig. 3.

This is quite remarkable, as the fluid properties change dramatically as the fluid cools down or heats up. In particular for the highest temperatures, the density and viscosity change by over 70% as the fluids passes through the heat exchanger. Experimental studies on the pressure drop of a supercritical turbulent flow being heated in a tube showed a strong dependency of the friction factor on the local fluid properties. A number of correlations have been proposed which use a correction factor to account for the local properties at the wall. For an overview, see Pioro et al. (2004). However, there are strong discrepancies between the different correlations, indicating a need for more research. It seems that for PHE the strong mixing and geometrically triggered turbulence, and the resulting pressure drops, outweighs the impact the local property variations have on the pressure drop.

CONCLUSIONS

As a first exploratory study, a standard plate heat exchanger design from SWEP (B16DW with 14 parallel channels) is studied here using supercritical Freon R23. This fluid is a scaling fluid for supercritical water. The pressure drop was determined for a varying flow rate and for an isothermal flow as well as for varying inlet temperature. This measured value was converted to a friction factor. The results indicate that despite the strong property variations which occur, the friction factors determined for flows with strongly varying properties, agree well with those for an isothermal flow. This is in contrast with earlier published findings for the friction factor of in-tube turbulent supercritical fluids.

ACKNOWLEDGEMENTS

The authors would like to express gratitude to the Netherlands Organization for Scientific Research (NWO), project number 680-47-119 and to the EU FW7 THINS project, which provided support for the current study.

REFERENCES

Arsenyeva, O. Tovazhnyansky, L. Kapustenko, P., Perevertaylenko, O., Khavin, G., 2011, *Investigation of the new corrugation pattern for low pressure plate condensers,* Applied Thermal Engineering, 31, pp. 2146-2152

Buongiorno, J., MacDonald, P.E., *Supercritical water reactor (SCWR), progress report for the FY-O3 Generation IV R&D activities for the development of the SCWR in the U.S.*, Report INEEL/EXT-03-01210, 38 pages, 2003.

Cha, J.E., Lee, T.H., Eoh, J.H., Seong, S.H., Kim, S.O., Kim, D.E., Kim, M.H., Kim, T.W., Suh, K.Y., 2009, *Development of a supercritical CO2 Brayton energy conversion system coupled with a sodium fast reactor*, Nuclear Engineering and Technology, 41, pp. 1025-1044

Ciofalo, M., Stasiek, J.A., Collins, M.W., 1996, *Investigation of flow and heat transfer in corrugated passages. Part II*, Int. J. Heat Mass Transfer, 39, pp. 165–192.

Claesson, J., 2004, *Thermal and hydraulic performance of compact brazed plate heat exchangers operating as evaporators in domestic heat pumps,* Ph.D. Thesis, Royal Institute of Technology, KTH, Stockholm

Dovic, D., Palm B., Švaić, S., (2009) *Generalized correlations for predicting heat transfer and pressure drop in plate heat exchanger channels of arbitrary geometry,* International Journal of Heat and Mass Transfer, 52**,** pp. 4553–4563.

Focke, W.W., 1983, *Turbulent convective transfer in plate heat exchangers,* International Communications in Heat and Mass Transfer, 10, pp. 201-210.

Freund, S. Kabelac, S., 2010, *Investigation of local heat transfer coefficients in plate heat exchangers with temperature oscillation IR thermography and CFD*, International Journal of Heat and Mass Transfer, 53, pp. 3764-3781

Khan, T.S., Khan, M.S., Chyu, C.M., Ayub, Z.H., 2010, *Experimental investigation of single phase convective heat transfer coefficient in a corrugated plate heat exchanger for multiple plate configurations,* Applied Thermal Engineering, 30**,** pp. 1058–1065.

Kim, M.H., Pettersen, J., Bullard, C.W., 2003, *Fundamental process and system design issues in CO2 vapor compression systems,* Progress in Energy and Combustion Science, 30, pp. 119-174.

Malek Abbaslou, R.M., Soltan Mohammadzadeh, J.S., Dalai, A.K., 2009, *Review on Fisher-Tropsch synthesis in supercritical media*, Fuel Processing Technology, 90, pp. 849-856.

Moffat, R. 1988, *Describing the uncertainties in experimental results*, Experimental and Thermal Fluid Science, 1, pp. 3-17

NIST REFPROP, reference fluid thermodynamic and transport properties, U.S. Department of Commerce, Washington DC (2007) NIST standard reference database 23, version 8.0

Pioro, I., Duffey, R.B., Dumouchel, T.J., 2004, *Hydraulic resistance of fluids flowing in channels at supercritical pressures (survey)*, Nuclear Engineering and Design 231, 187-197

Rohde, M., Marcel, C.P., T'Joen C., Class, A., Van der Hagen, T.H.J.J., 2011, *Downscaling a supercritical water loop for experimental studies on system stability*, International Journal of Heat and Mass Transfer 54, pp. 65-74

Schmieder, H., Abeln, J., 1999, *Supercritical water oxidation: state of the art*, Chemical Engineering & Technology 22, 903-908.

Schuster A., Karellas S. and Aumann R., 2010, *Efficiency Optimization Potential in Supercritical Organic Rankine Cycles*, Energy, 35, pp. 1033-39.

Shah, R.K., Focke, W.W., 1988, Plate heat exchangers and their design theory, in Heat Transfer Equipment Design, Hemisphere Publishing Corp., Washington D.C., pp. 227-254

Shah, R.K., Sekulic, D.P., 2003, *Fundamentals of heat exchanger design*, John Wiley & Sons, Inc., Hoboken, New Jersey, 1st edition

Stasiek, J.A., Collins, M. W., Ciofalo, M., Chew, P.E., 1996, *Investigation of flow and heat transfer in corrugated passages. Part I,* Int. J. Heat Mass Transfer 39, pp. 149–164.

Susta, M.R., 2004, *Supercritical and Ultra-Supercritical Power Plants – SEA's Vision or Reality*, Proceedings of POWERGEN ASIA 2004, pp. 1-23.